Springer

KSME

Journal of Mechanical Science and Technology 31 (11) (2017) 5407~5414
www.springerlink.com/content/1738-494x(Print)/1976-3824(Online)
DOI 10.1007/s12206-017-1035-y

Effects of surface nanostructures on self-cleaning and anti-fogging characteristics of transparent glass †

Taeho Son[1], Eunjin Yang[1], Eusun Yu[2], Kyu Hwan Oh[2], Myoung-Woon Moon[3,*] and Ho-Young Kim[1,4,*]

[1]*Department of Mechanical and Aerospace Engineering, Seoul National University, Seoul 08826, Korea*
[2]*Department of Materials Science and Engineering, Seoul National University, Seoul 08826, Korea*
[3]*Computational Science Research Center, Korea Institute of Science and Technology, Seoul 02792, Korea*
[4]*Urban Data Science Laboratory, SNU BDI, Seoul 06324, Korea*

(Manuscript Received February 25, 2017; Revised June 13, 2017; Accepted July 12, 2017)

Abstract

Nanostructured transparent glass surfaces with self-cleaning and anti-fogging properties were fabricated using a non-lithographic, anisotropic etching technique. The superhydrophilic glass surface was achieved by nanostructuring pre-deposited SiO_2 film in a glow discharge chamber. For superhydrophobicity, the surface energy of the nanostructured glass was lowered by treatment with 1*H*,1*H*,2*H*,2*H*-perfluorooctyl trichlorosilane. The self-cleaning and anti-fogging behavior was compared for glasses with different wettabilities by measuring the optical transmittance as well as the surface morphology and contact angles. In measuring the anti-fogging behavior, we included the effects of air flow impinging on the glass surface to emulate many practical situations. The superhydrophobic glass was superior to the superhydrophilic glass when considering both the self-cleaning and anti-fogging behavior with durability, particularly under air flow. The work can be used to fabricate transparent glass products for which minimizing surface contamination is crucial, e.g., eyeglasses, solar cells, and optical instruments.

Keywords: Self-cleaning; Anti-fogging; Nanostructure; Superhydrophobic; Superhydrophilic

1. Introduction

On a self-cleaning surface, contaminant particles are collected by water droplets and then removed as the droplets roll off the surface [1]. In nature, one can find various examples of self-cleaning surfaces including lotus leaves [1], water strider legs [2, 3], and cicada wings [4, 5]. The self-cleaning property is closely associated with the superhydrophobicity of the surface, resulting from surface roughness covered with chemical substances of low surface energies [1].

Another surface property of growing interest is anti-fogging. Fogging results from droplets with diameters larger than 190 nm, or half of the shortest wavelength (380 nm) of visible light, on the surface because they scatter visible light [6]. Either superhydrophobic or superhydrophilic treatment can prevent those droplets from forming on the surface. Superhydrophobicity caused by structures of micro or nanometer scales on the surface inhibits condensation or growth of droplets. Some insects, such as mosquitos and green bottle flies, have superhydrophobic eyes with strong anti-fogging properties [6, 7]. On superhydrophilic surfaces, a transparent thin water film arises as a result of condensation instead of water drops which scatter light [8-12].

In addition to the foregoing surface characters, one should consider the following aspects for practical applications. First, many surfaces including metal oxides [13], glass [14], silicon [15], and graphene [16] lose their hydrophilicity in a few days due to airborne contaminants covering the surface. For applications of functional transparent surfaces including optical instruments, display windows, and outdoor uses such as solar panels, vehicles, and wearable devices, long-term sustainability of self-cleaning and anti-fogging properties are essential. Second, in many artificial superhydrophobic surfaces, the structures added to increase the surface roughness are made from a different material than the substrate, leading to intrinsic problems with structural durability, such as detachment of the added structure or capillary coalescence upon exposure to water [17-21]. Only a few surfaces have been reported with micro or nanostructures made from the same material as the substrate like glass [9, 22-24]. Third, for good transparency, it is necessary for the glass to have nanostructures, as microstructured glass is opaque [22]. However, nanostructuring of glass surface generally requires many additional fabrication

*Corresponding author. Tel.: +82 2 958 5487 (M.-W. Moon), 82 2 880 9286 (H.-Y. Kim), Fax.: +82 2 880 9287 (H.-Y. Kim)
E-mail address: mwmoon@kist.re.kr, hyk@snu.ac.kr
† Recommended by Associate Editor Taesung Kim

Table 1. As-placed or static (θ_S), critical advancing (θ_A), and critical receding (θ_R) contact angles of water on the glass surfaces used in the self-cleaning and anti-fogging experiments.

Glass surface	Fabrication method	Surface structure	θ_S (deg)	θ_A (deg)	θ_R (deg)
Superhydrophobic	CF_4 etching + PFOTS coating	Nanostructured	168 ± 3	170 ± 3	167 ± 3
Hydrophobic	Piranha treatment + PFOTS coating	Smooth	103 ± 1	107 ± 1	78 ± 1
Hydrophilic	Piranha treatment	Smooth	2 ± 1	3 ± 1	0 ± 1
Superhydrophilic	CF_4 etching + Washing in water	Nanostructured	1 ± 1	2 ± 1	0 ± 1

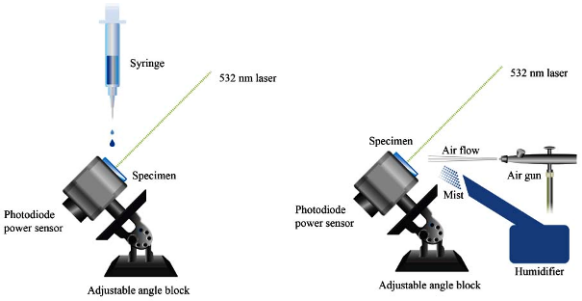

Fig. 1. Experimental setups for (a) self-cleaning; (b) anti-fogging tests.

steps [9, 23, 24].

In this study, we fabricated nanostructured glass with extreme water-affinity or water-repellency by modifying a non-lithographic, anisotropic etching method [25]. We used a glow discharge method of Plasma-enhanced chemical vapor deposition (PECVD) as it is a facile fabrication method applicable for large-scale production. Only two steps are required, deposition and etching, to fabricate nanostructured glass. Furthermore, only water is needed to remove by-product after etching, instead of toxic chemicals [9, 23, 24]. The self-cleaning and anti-fogging properties and durability of the glasses were tested and compared considering the effects of external air flow.

2. Experimental

2.1 Fabrication method

We prepared four types of glass surfaces: hydrophilic, hydrophobic, superhydrophilic, and superhydrophobic. The fabrication schemes and resulting contact angles of water for each surface are listed in Table 1. To prepare the hydrophilic surface without organic residues, the glass (microscope slide, Marienfeld, Germany) was immersed in a piranha solution, a 3:1 mixture of sulfuric acid (ACS reagent, 95.0–98.0 %, Sigma-Aldrich) and a hydrogen peroxide solution (ACS reagent, 30 wt% in H_2O, Sigma-Aldrich) for 30 min [26].

To prepare the hydrophobic surface, the glass was first immersed in the same piranha solution for 30 min. Then 1*H*,1*H*,2*H*,2*H*-perfluorooctyl trichlorosilane (PFOTS; 97 %, Sigma-Aldrich) was used to reduce the surface energy. The glass was exposed to PFOTS vapor for 120 s, thoroughly washed with acetone (ACS reagent, ≥ 99.5 %, Sigma-Aldrich), and then dried with nitrogen gas.

To fabricate the superhydrophilic surface, a 1 μm thick SiO_2 layer was deposited on the glass in a PECVD chamber with a mixture of N_2O and SiH_4 gas. The glass was then etched using a glow discharge of CF_4 gas for 40 min to obtain a nanostructured surface. The gas pressure and bias voltage were maintained at 30 mTorr and -600 V, respectively. Subsequently, the etched glass was immersed in water to remove metal fluorides generated by the etching process off the surface and then dried with pure nitrogen gas [25]. There was no difference in the morphology of the nanostructures before and after immersion in water.

To obtain the superhydrophobic surface, nanostructured glass was fabricated using the same method as for the superhydrophilic glass. Then the glass was immersed in the piranha solution for 30 min and coated with PFOTS by vapor deposition, as described above. We confirmed that the CF_4 etching time of 40 min and the PFOTS vapor deposition time of 120 s resulted in the maximum static contact angles as will be delineated below.

Field-emission scanning electron microscopy (FESEM; SUPRA 55VP, Carl Zeiss) was used to observe the nanostructures on the glass substrates. The critical advancing (θ_A) and receding contact angles (θ_R) were measured by increasing or decreasing the drop volume with an aid of a syringe needle immersed in the drop until the contact line started to move [27]. The contact angles of DI (deionized) water, ethylene glycol (ReagentPlus®, 99 %, Sigma-Aldrich), and hexadecane (anhydrous, ≥ 99.5 %, Sigma-Aldrich) were measured from the optical images of each sessile drop 4.2 μl in volume based on the perturbation solution of the Bashforth-Adams equation [28]. A digital camera (D300S, Nikon) was used to obtain optical images of the sessile drop and the glass surfaces.

2.2 Experimental setup

The experimental setups used to characterize the self-cleaning and anti-fogging behavior of the glasses are shown in Fig. 1. To quantify the self-cleaning performance of the glasses with different wettability, we compared the optical transmittance before and after they contact DI water drops, as shown in Fig. 1(a). Silicon carbide particles (SiC; ~400 mesh particle size, Sigma-Aldrich) were used as an artificial contaminant, due to its similarity in size and wettability to natural dirt [29]. Glass contaminated with SiC particles was tilted at 45°, the angle used in many industrial weathering tests (ISO 1514:2004E) [29, 30]. Water droplets of 2 mm in diameter were dispensed every 10 s from a syringe suspended 40 mm above the center of the tilted glass with impact velocity of 0.9 m/s. The optical transmittance under the irradiation of beam

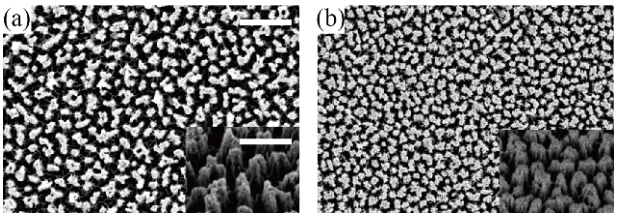

Fig. 2. Top-view and 40° tilted-view (inset) FESEM images of the surfaces of nanostructured glass with two CF_4 plasma etching times: (a) 40 min; (b) 60 min. Scale bars, 1 μm and 500 nm (inset).

from a 2 W, 532 nm Diode-pumped solid-state (DPSS) laser was measured in the center of the glass using a Si photodiode power sensor (PM121D, Thorlabs).

To quantify the anti-fogging performance, the same stage was used with an ultrasonic humidifier instead of a syringe to supply fog, as shown in Fig. 1(b). The humidity before the test was 25 % and the temperature of the stage was 22 °C. Fog was blown towards the center of the glass through a tube with a 10 mm diameter for initial 2 min. The distance between the center of the glass and the tube was set to be 40 mm to supply sufficient fog while minimizing the effect of the fog stream on the laser. To investigate the unfogging capability of external gas flow on each type of surface, N_2 gas flow was applied to the glass surface with the velocity of 10 m/s as measured using an air velocity meter (Velocicalc Model 8346, TSI) from the beginning of the corresponding experiments.

3. Results and discussion

3.1 Optimized fabrication conditions of superhydrophobic surface

We varied the durations of CF_4 plasma etching and PFOTS vapor deposition to seek the optimal conditions for high static contact angles for the liquids used in this work. It was reported that the CF_4 plasma etching lasting shorter than 35 min did not completely remove the SiO_2 layer off the surface [25]. In Fig. 2, we show FESEM images of the nanostructured glass surfaces produced through CF_4 plasma etching treatment of 40 and 60 min duration. We see that as the plasma etching lasts longer, the nanopillars formed on the surface are denser, indicating a higher area fraction of solid in contact with a drop sitting on it. As the Cassie-Baxter equation states, the apparent contact angle θ_r of a liquid drop on a rough surface is given by

$$\cos\theta_r = f_1\cos\theta_e - f_2, \quad (1)$$

where θ_e is the equilibrium contact angle, and f_1 and $f_2 = 1 - f_1$ are the solid fraction and air fraction of the rough surface, respectively. To achieve high contact angles (θ_r) of liquids on nanostructured glass, it is necessary to decrease the solid fraction and increase the air fraction. The measurement results of static contact angles for different fabrication conditions, plotted in Fig. 3, indeed show that CF_4 plasma etching time of 40 min (blue symbols) results in higher contact angles than from 60 min (red symbols) of etching.

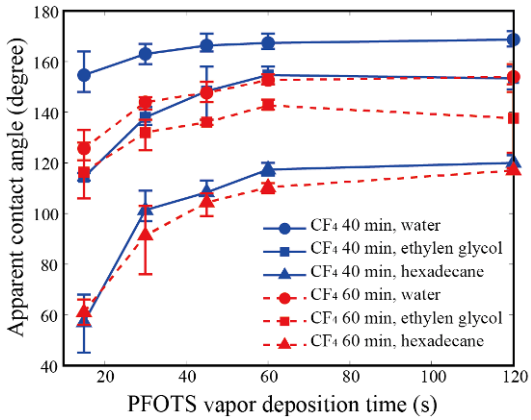

Fig. 3. Effects of CF_4 plasma etching time and PFOTS vapor deposition time on static contact angles of water (circle), ethylene glycol (square), and hexadecane (triangle) drops on PFOTS-treated nanostructured glasses. Blue and red symbols correspond to CF_4 plasma etching times of 40 and 60 min, respectively.

Fig. 3 also shows that the contact angles increase with PFOTS vapor deposition time but almost saturate near 120 s for all the liquids. We note that the apparent contact angles of the superhydrophobic surface are fairly large for the liquids other than water as well, so that θ_r reaches 168°, 153° and 120° for water, ethylene glycol and hexadecane, respectively. This implies that our relatively simple plasma-based fabrication procedure, which has a great potential for large area treatment, can lead to omniphobic surfaces. Considering these observations, we selected a CF_4 plasma etching time of 40 min for both superhydrophilic and superhydrophobic nanostructured glasses, and a PFOTS vapor deposition time of 120 s for superhydrophobic glass fabrication.

3.2 Surface durability

Fig. 4 shows the static contact angles of a water drop on the glasses exposed to an indoor environment over a period of 42 days. The temperature and humidity were kept at 22±1 °C and 21-25 %, respectively. The contact angle of the superhydrophobic glass was kept over 160°, demonstrating its long-term durability. The hydrophobic glass also showed a fairly good long-term stability. However, the contact angle of the hydrophilic glass drastically increased from 2° to 45° after seven days. Then it increased slowly afterwards. Because the surface OH groups which determine wettability of an oxide surface works as adsorption sites for organic substances in the atmosphere, the contact angle of the hydrophilic glass increased by capturing airborne contaminants [13, 14]. The increased contact angle after one week in our experiment (45°) was higher than the angle (30°) observed in the similar experiments of Takeda et al. [14]. In our case, the glass surfaces were directly exposed to an indoor environment, whereas the samples of Takeda et al. were stored in a desiccator where the temperature and humidity were controlled [14]. Hence, our

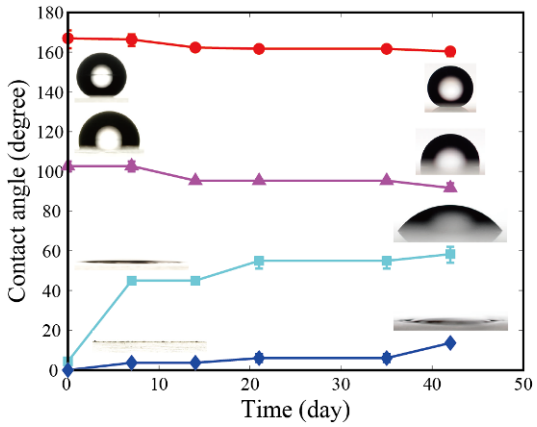

Fig. 4. Static contact angles of water over time on superhydrophobic (circles), hydrophobic (triangles), hydrophilic (squares), and superhydrophilic (diamonds) glass exposed to an indoor environment.

glass surfaces were more prone to contamination by organic substances or dust, resulting in the severer increase in the contact angle. The contact angle of superhydrophilic glass was initially almost 0° due to the surface roughness and the effect of the surface OH groups. The contact angle of the superhydrophilic glass gradually increased reaching 14° in 42 days. This indicates a slow degradation of the superhydrophilicity.

3.3 Self-cleaning test

The self-cleaning properties of the glass surfaces with different wettabilities are compared in Figs. 5 and 6. Fig. 5 shows the change of transmittance of the four different glass surfaces under the experiment depicted in Fig. 1(a). Before contaminated with SiC particles, the transmittance of the superhydrophobic, hydrophobic, hydrophilic, and superhydrophilic glasses were 94, 90, 90 and 94 %, respectively. Note the high transmittance values of the glasses even after nanostructuring. After contamination with SiC particles, the transmittance of all the kinds of glass surfaces reduced to about 63 %. As water drops were dropped onto the surfaces (at a spot where the transmittance is measured) tilted 45° from a horizontal, the transmittance of the superhydrophobic and hydrophobic glasses was recovered to approximately 90 % by the first drop. The transmittance of the other glasses was not fully recovered until the second drop arrived.

Fig. 6 shows optical images of the four different glass surfaces before and after the self-cleaning experiments. The lighter areas in the "after" images show where the water has removed the SiC particles. When a water drop collided with the superhydrophobic glass surface, it picked up SiC particles and removed them as it bounced off. There was no residual water on the surface after the test, as shown in Fig. 6(a). A water drop on the hydrophobic glass surface also collected the SiC particles, but it slid down and was retained at the bottom edge of the glass [31], as shown in Fig. 6(b). The drop failed to disengage from the surface because the hydrophobic glass

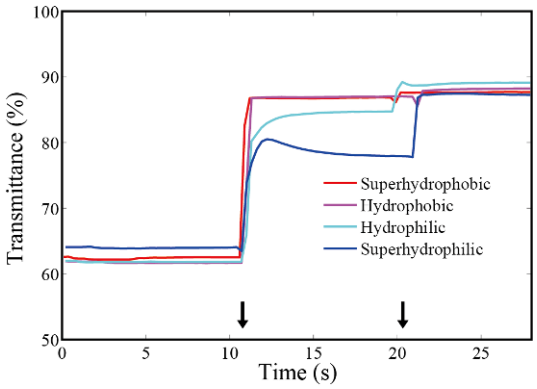

Fig. 5. Change of the optical transmittance of a 532 nm laser through superhydrophobic, hydrophobic, hydrophilic, and superhydrophilic glasses contaminated with SiC particles. The arrows indicate the impact of a water drop.

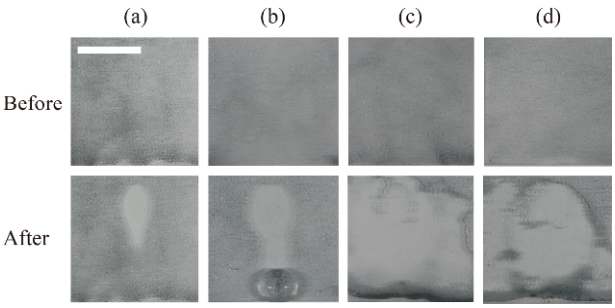

Fig. 6. Optical images of (a) superhydrophobic; (b) hydrophobic; (c) hydrophilic; (d) superhydrophilic glass contaminated with SiC particles before (t = 0) and after (t = 60 s) the self-cleaning test with two drops of water. The scale bar, 10 mm.

had a lower contact angle and higher contact angle hysteresis (θ_A - θ_R) than the superhydrophobic glass.

Although the transmittance of all the glass surfaces was recovered after two drops impacted on the surfaces, the optical images of the hydrophilic and superhydrophilic surfaces are quite different from the other surfaces. On both the hydrophilic (Fig. 6(c)) and superhydrophilic (Fig. 6(d)) glass surfaces, water films were formed and their boundaries were re-contaminated by a mixture of water and SiC particles. However, the center of the glasses, where the water drops hit and the transmittance measurements were undertaken, was clean.

3.4 Anti-fogging test

The change of optical transmittance of the four different glasses subjected to fogging with and without external gas flow (Fig. 1(b)) are shown in Fig. 7. Images of the corresponding surfaces are shown in Fig. 8. The transmittance of the fogged superhydrophobic and hydrophobic glasses without external flow drastically decreased to about 40 % and 30 %, respectively. These values are much lower than those of superhydrophilic (78 %) and hydrophilic (62 %) surfaces since the condensed drops on the superhydrophobic and hydropho-

bic surfaces scatter light, as shown in Fig. 8(a). On superhydrophilic and hydrophilic surfaces, water films are formed and flow down. In particular, the water collected on the superhydrophilic surface quickly spreads by hemiwicking [31], which appears to lead to the uniform film thickness and less deteriorated transmittance.

Although the thickness of liquid wicking into the gaps of microscale protrusions is approximated to be the height of the micro-asperities [32, 33], the thickness of liquid films spreading on surfaces with nanoroughness has not been characterized yet. In particular, a film tends to grow while flowing down when fog droplets are supplied as in this test. A further study is called for to measure the film thickness on the superhydrophilic nanostructured surfaces.

As the fog supply is stopped at 2 min, all the glasses recovered their transmittance to original values. The recovery of the superhydrophilic glass is almost immediate, reconfirming the fairly uniform thickness of water film. It takes from about 7 to 9 min for the other surfaces to recover the transmittance. For the hydrophilic surface, it is a time taken for initially irregular film thickness to become uniform by slow drainage. For the superhydrophobic and hydrophobic surfaces, it is a time for small drops on the surfaces either to evaporate or roll down.

When the external gas flow was applied (Fig. 7(b)), the superhydrophilic glass exhibited the smallest decrease of transmittance, implying a further decrease of film thickness. The hydrophilic glass showed the most significant drop of transmittance, a different behavior from Fig. 7(a). It is because a thick water film on the surface rippled under the influence of external gas flow, as clearly shown in Fig. 8(b). The hydrophobic glass exhibited the similar extent of transmittance reduction as when external gas flow was absent, hinting at insignificant help of gas flow in removing water drops. The superhydrophobic glass benefited greatly from the external flow as the transmittance dropped only to about 77 % as compared with 40 % when the flow was absent.

To understand different degree of effects of external gas flow on transmittance change of hydrophobic and superhydrophobic glass surfaces, we estimate a diameter of drop that can be removed by external flow. To dislodge a drop with diameter D, the drag force due to external flow needs to overcome the capillary force arising from the contact angle hysteresis [34, 35]:

$$\frac{1}{2}C_D\rho_a V^2\left(\frac{\pi D^2}{4}\right) > b\sigma\left(\cos\theta_A - \cos\theta_R\right). \quad (2)$$

The left-hand side of the inequality corresponds to the drag force, where C_D is the drag coefficient, ρ_a and V are the density and velocity of the air, respectively. The right-hand side is the capillary force, where b is the diameter of the contact area of the drop, and σ is the surface tension of the water. Based on the spherical cap profile of drop, we can approximate b as $D\sin\theta_s$. Then we get

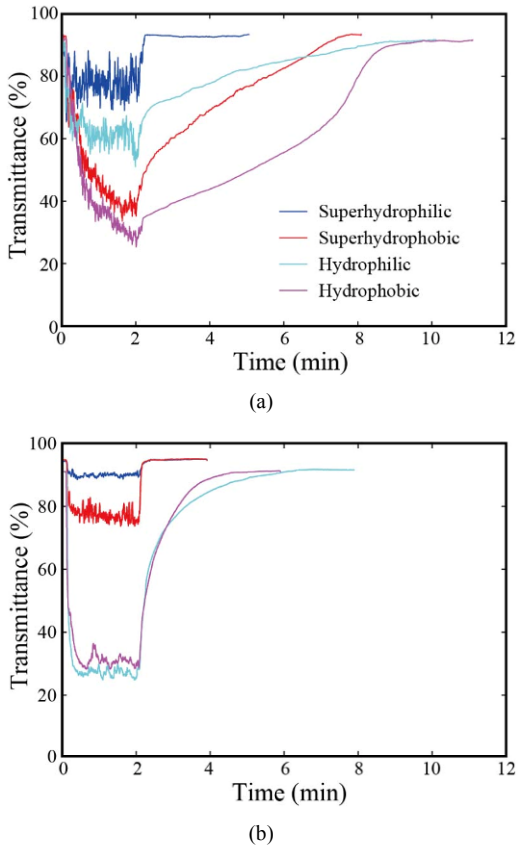

Fig. 7. Evolution of optical transmittance of 532 nm laser through superhydrophobic, hydrophobic, hydrophilic, and superhydrophilic glasses subjected to fogging (a) without; (b) with air flow of 10 m/s.

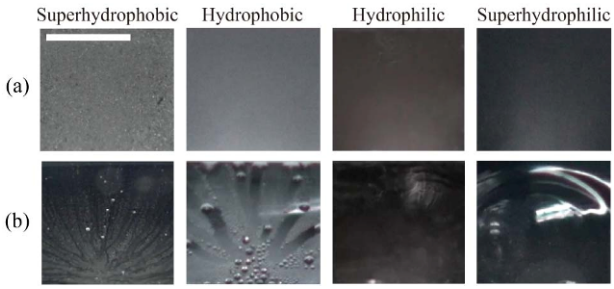

Fig. 8. Optical images of the anti-fogging test results on superhydrophobic, hydrophobic, hydrophilic, and superhydrophilic glasses subjected to fogging (a) without; (b) with external air flow of 10 m/s at t = 90 s. The radiating transparent patterns of superhydrophobic and hydrophobic surfaces in (b) correspond to the paths of water drops pushed by impinging gas flow. The scale bar, 10 mm.

$$D > \frac{8\sigma\sin\theta_S\left(\cos\theta_A - \cos\theta_R\right)}{\pi C_D\rho_a V^2}. \quad (3)$$

We see that the surface with a higher contact angle and lower contact angle hysteresis would remove smaller drops from the surface under external flow. Using ρ_a = 1.3 kg/m^3, V = 10 m/s, and the contact angles in Table 1, the estimated minimum drop diameters removable from the surface are of

the order of 1 μm and 1 mm on the superhydrophobic and the hydrophobic surface, respectively. Therefore, drops growing larger than micrometric sizes are quickly removed from the superhydrophobic surface, while drops can grow to millimetric sizes on the hydrophobic surface before being shed off.

Under external gas flow, the transmittance for each surface in Fig. 7(b) was recovered faster than that in Fig. 7(a). The recovery for the hydrophilic glass is supposed to be due to augmented evaporation of water film by gas convection. The fast recovery of both the hydrophobic and superhydrophobic surfaces is mainly due to removal of water droplets off the surfaces by drag of gas flow as quantified above.

3.5 Selection of better surface

The superhydrophobic and hydrophobic glasses showed complete and partial self-cleaning behavior, respectively. The hydrophilic and superhydrophilic glasses were shown to be re-contaminated by mixture of the water and contaminants in self-cleaning test. Since our experiments were conducted on small surfaces (~6 cm^2), larger surface areas of hydrophilic and superhydrophilic glasses would be more prone to re-contamination of the water-particle mixture. After evaporation of the water, it was more difficult to remove the coagulated contaminants from the glass surface by tilting or blowing. Furthermore, it was reported that when glass was exposed to outdoor conditions, degradation of the optical transmittance occurs due to dust accumulation [36]. In some applications including the side mirror glasses of automobiles, a double layer of SiO_2 and TiO_2 is deposited to recover glass hydrophilicity by UV light irradiation [37]. However, considering the danger of re-contamination by water and resistance to dust accumulation, we can conclude that the superhydrophobic glass would be the best self-cleaning surface.

Although superhydrophobic and hydrophobic glasses exhibited poorer anti-fogging properties than hydrophilic surfaces without external flow, the optical transmittance of superhydrophobic glass exposed to gas stream reached a similar value to the superhydrophilic glass without the wind. Based on experimental observation and theoretical analyses, we also found that superhydrophobic glass with external flow showed fast elimination of small drops as compared with the hydrophobic glass. Superhydrophilic glass showed the highest optical transmittance with or without external flow. However, the contact angle of superhydrophilic glass gradually increases with time, which will naturally lead to degraded anti-fogging behavior with time. Hence, considering both self-cleaning and anti-fogging performances for long-term use, we suggest that the optimal functional glass would be the superhydrophobic nanostructured glass. Here we tested only soda-lime glass with different wettabilities, but contact angles of water on other commercial glasses such as boroaluminosilicate glass and a vitreous silica glass similarly increased after one week [14]. Therefore, other commercial glasses with different wettability are expected to show similar aging behavior of self-cleaning and anti-fogging properties as tested here.

4. Conclusions

We fabricated nanostructured transparent glasses using non-lithographic, anisotropic etching, and investigated the effects of the wettability of the glass on the self-cleaning and anti-fogging behavior. After the self-cleaning test with glasses of different wettabilities, superhydrophilic and hydrophilic glass surfaces had residual water drops or mixture of water and dirt, which may cause secondary effects such as coagulation of contaminants after evaporation of the water. The superhydrophobic glass showed outstanding self-cleaning properties and the hydrophobic glass showed partial self-cleaning behavior where sufficient kinetic energy of the water droplet was necessary for it to slide down the surface. While previous researches examined the anti-fogging properties in the absence of ambient air flow [6-8], we showed that nanostructured superhydrophobic glass subjected to external flow had anti-fogging behavior. The superhydrophilic glass showed good performance of anti-fogging with or without external flow. On the hydrophilic glass surfaces, an external flow reduced the optical transmittance by generating ripples of water film that scatter light. Considering both the self-cleaning and anti-fogging properties with durability, superhydrophobic glass is suggested to be superior to superhydrophilic glass. The process we developed in this work can be used to fabricate glass products for eyeglasses, solar cells, vehicles, and optical instruments, where minimizing surface contamination is crucial.

Acknowledgments

This work was supported by National Research Foundation of Korea (Grant Nos. 2016901290 and 2016913167) and Disaster and Safety Management Institute, Ministry of Public Safety and Security of Korea (MPSS-CG-2016-02) via SNU IAMD.

References

[1] W. Barthlott and C. Neinhuis, Purity of the sacred lotus, or escape from contamination in biological surfaces, *Planta,* 202 (1997) 1-8.

[2] X. Gao and I. Jiang, Water-repellent legs of water striders, *Nature,* 432 (2004) 36.

[3] X.-Q. Feng, X. Gao, Z. Wu, L. Jiang and Q.-S. Zheng, Superior water repellency of water strider legs with hierarchical structures: experiments and analysis, *Langmuir,* 23 (2007) 4892-4896.

[4] T. Wagner, C. Neinhuis and W. Barthlott, Wettability and contaminability of insect wings as a function of their surface sculptures, *Acta Zool,* 77 (1996) 213-226.

[5] K. M. Wisdom, J. A. Watson, X. Qu, F. Liu, G. S. Watson and C.-H. Chen, Self-cleaning of superhydrophobic surfaces by self-propelled jumping condensate, *Proc. Natl. Acad. Sci.,*

USA, 110 (2013) 7992-7997.
[6] X. Gao, X. Yan, X. Yao, L. Xu, K. K. Zhang, J. Zhang, B. Yang and L. Jiang, The dry-style antifogging properties of mosquito compound eyes and artificial analogues prepared by soft lithography, *Adv. Mater,* 19 (2007) 2213-2217.
[7] Z. Sun, T. Liao, K. Liu, L. Jiang, J. H. Kim and S. X. Dou, Fly-eye inspired superhydrophobic anti-fogging inorganic nanostructures, *Small,* 10 (2014) 3001-3006.
[8] F. C. Cebeci, Z. Z. Wu, L. Zhai, R. E. Cohen and M. F. Rubner, Nanoporosity-driven superhydrophilicity: a means to create multifunctional antifogging coatings, *Langmuir,* 22 (2006) 2856-2862.
[9] K.-C. Park, H. J. Choi, C.-H. Chang, R. E. Cohen, G. H. McKinley and G. Barbastathis, Nanotextured silica surfaces with robust superhydrophobicity and omnidirectional broadband supertransmissivity, *ACS Nano,* 6 (2012) 3789-3799.
[10] C. S. Thompson, R. A. Fleming and M. Zou, Transparent self-cleaning and antifogging silica nanoparticle films, *Sol. Energ. Mat. Sol. C,* 115 (2013) 108-113.
[11] P. Chevallier, S. Turgeon, C. Sarra-Bournet, R. Turcotte and G. Laroche, Characterization of multilayer anti-fogging coating, *ACS Appl. Mater. Interfaces*, 3 (2011) 750-758.
[12] M. W. England, C. Urata, G. J. Dunderdale and A. Hozumi, Anti-fogging/self-healing properties of clay-containing transparent nanocomposite thin films, *ACS Appl. Mater. Interfaces,* 8 (2016) 4318-4322.
[13] S. Takeda, M. Fukawa, Y. Hayashi and K. Matsumoto, Surface OH group governing adsorption properties of metal oxide films, *Thin Solid Films,* 339 (1999) 220-224.
[14] S. Takeda, K. Yamamoto, Y. Hayasaka and K. Matsumoto, Surface OH group governing wettability of commercial glasses, *J. Non-Cryst. Solids,* 249 (1999) 41-46.
[15] J. Ruzyllo, Assessment of the progress in gas-phase processing of silicon surfaces, *ECS J. Solid State Sci. Technol.,* 3 (2014) N3060-N3063.
[16] Z. Li, Y. Wang, A. Kozbial, G. Shenoy, F. Zhou, R. McGinley, P. Ireland, B. Morganstein, A. Kunkel, S. P. Surwade, L. Li and H. Liu, Effect of airborne contaminants on the wettability of supported graphene and graphite, *Nat. Mater.,* 12 (2013) 925-931.
[17] K. K. S. Lau, J. Bico, K. B. K. Teo, M. Chhowalla, G. A. J. Amaratunga, W. I. Milne, G. H. McKinley and K. K. Gleason, Superhydrophobic carbon nanotube forests, *Nano. Lett.,* 3 (2003) 1701-1705.
[18] C. H. Lee, J. Drelich and Y. K. Yap, Superhydrophobicity of boron nitride nanotubes grown on silicon substrates, *Langmuir,* 25 (2009) 4853-4860.
[19] J. Fan and Y. Zhao, Nanocarpet effect induced superhydrophobicity, *Langmuir,* 26 (2010) 8245-8250.
[20] S. E. Lee, H.-J. Kim, S.-H. Lee and D.-G. Choi, Superamphiphobic surface by nanotransfer molding and isotropic etching, *Langmuir,* 29 (2013) 8070-8075.
[21] T.-H. Kim, S. Kim and H.-Y. Kim, Evaporation-driven clustering of microscale pillars and lamellae, *Phys. Fluids,* 28 (2016) 022003.
[22] M. S. Ahsan, F. Dewanada, M. S. Lee, H. Sekita and T. Sumiyoshi, Formation of superhydrophobic soda-lime glass surface using femtosecond laser pulses, *Appl. Surf. Sci.,* 265 (2013) 784-789.
[23] J. Son, L. K. Verma, A. J. Danner, C. S. Bhatia and H. Yang, Enhancement of optical transmission with random nanohole structures, *Opt. Express,* 19 (2011) A35-A40.
[24] L. K. Verma, M. Sakhuja, J. Son, A. J. Danner, H. Yang, H. C. Zeng and C. S. Bhatia, Self-cleaning and anti-reflective packaging glass for solar modules, *Renewable Energ,* 36 (2011) 2489-2493.
[25] E. Yu, S. C. Kim, H. J. Lee, K. H. Oh and M.-W. Moon, Extreme wettability of nanostructured glass fabricated by non-lithographic anisotropic etching, *Sci. Rep.,* 5 (2015) 9362.
[26] F. Pintchovski, J. B. Price, P. J. Tobin, J. Peavey and K. Kobold, Thermal characteristics of the H_2SO_4-H_2O_2 silicon wafer cleaning solution, *J. Electrochem. Soc.,* 126 (1979) 1428-1430.
[27] P.-G. de Gennes, F. Brochard-Wyart and D. Quere, *Capillarity and wetting phenomena: Drops, bubbles, pearls, waves*, Springer, New York, USA (2004).
[28] S. Srinivasan, G. H. McKinley and R. E. Cohen, Assessing the accuracy of contact angle measurements for sessile drops on liquid-repellent surfaces, *Langmuir,* 27 (2011) 13582-13589.
[29] B. Bhushan, Y. C. Jung and K. Koch, Self-cleaning efficiency of artificial superhydrophobic surfaces, *Langmuir,* 25 (2009) 3240-3248.
[30] Y.-B. Park, H. Im, M. Im and Y.-K. Choi, Self-cleaning effect of highly water-repellent microshell structures for solar cell applications, *J. Mater. Chem.,* 21 (2011) 633-636.
[31] A. Lee, M.-W. Moon, H. Lim, W.-D. Kim and H.-Y. Kim, Water harvest via dewing, *Langmuir*, 28 (2012) 10183-10191.
[32] J. Kim, M.-W. Moon and H.-Y. Kim, Dynamics of hemiwicking, *J. Fluid Mech.,* 800 (2016) 57-71.
[33] J. Kim, M.-W. Moon, K.-R. Lee, L. Mahadevan and H.-Y. Kim, Hydrodynamics of writing with ink, *Phys. Rev. Lett.,* 107 (2011) 264501.
[34] G. McAlister, R. Ettema and J. S. Marshall, Wind-driven rivulet breakoff and droplet flows in microgravity and terrestrial-gravity conditions, *J. Fluids Eng.,* 127 (2005) 257-266.
[35] H.-Y. Kim, H. J. Lee and B. H. Kang, Sliding of liquid drops down an inclined solid surface, *J. Colloid Interface Sci.,* 247 (2) (2002) 372-380.
[36] H. K. Elminir, A. E. Ghitas, R. H. Hamid, F. El-Hussainy, M. M. Beheary and K. M. Abdel-Moneim, Effect of dust on the transparent cover of solar collectors, *Energ. Convers. Manage.,* 47 (2006) 3192-3203.
[37] M. Nakamura, M. Kobayashi, N. Kuzuya, T. Komatsu and T. Mochizuka, Hydrophilic property of SiO_2/TiO_2 double layer films, *Thin Solid Films,* 502 (2006) 121-124.

Taeho Son received his B.S. and M.S. degrees from Seoul National University in Mechanical and Aerospace Engineering. He is currently in Samsung Electronics. His research interests are microfluidics and mechatronics.

Ho-Young Kim received his B.S. degree from Seoul National University and M.S. and Ph.D. degrees from MIT all in mechanical engineering. He is now a Professor of mechanical engineering at Seoul National University. His research activities revolve around microfluid mechanics, bio-mimetics, and soft matter physics.